Heat and Mass MHD Convection of Nanofluid through an Inclined Permeable Channel with Thermal Radition

Achogo Wisdom Hezekiah (PhD) & Offor Temple Daniel (PhD)
Department of Mathematics/Statistics,
Ignatius Ajuru University of Education, P.M.B 5047 Rumuolumeni, Nigeria.
achogo64@gmail.com

D.O.I: 10.56201/ijasmt.v9.no1.2023.pg42.58

Abstract
Heat and Mass MHD convection of nanofluid is examined over an inclined porous channel with thermal radiation. Coupled partial differential equations were obtained for the momentum and temperature in view of the problem. These equations were analytically solved. The equations were converted to ordinary differential equations through a one term perturbation technique. The exact solutions for the ordinary differential equations were obtained and plotted to ascertain the effects of parameters variations on the velocity and temperature profiles. The effects of parameters variations were noted from the plots. It noted that increasing the magnetic field parameter and solutal Grashof number reduces and increases the velocity of the nanofluid respectively. Increase in the thermal radiation reduces the temperature while increase in the Peclet number correspondingly increases the temperature of the nanofluid.

Keywords: *Natural Convection, Porosity, Magnetohydrodynamics, Nanofluid*

I. INTRODUCTION

Warm conductivity assumes an essential part in warmness move upgrade. Traditional intensity switch liquids alongside water, ethylene glycol (EG), lamp fuel oil and ointment oils have negative warm conductivities contrasted with solids. Solids garbage anyway has better warm conductivities in contrast with customary warmth switch liquids. Choi (1995) in his spearheading compositions demonstrated that when a little amount of nanoparticles is added to normal base liquids, it will increment widely the warm conductivity of the base liquids notwithstanding their convective warmness move rate. This mix is known as nanofluids. All the more unequivocally, nanofluids are suspensions of nano-length trash in base liquids. Normally nanofluids incorporate explicit kinds of nanoparticles comprehensive of oxides, metals and carbides in for the most part base liquids like water, EG, propylene glycol and lamp oil. A few special bundles of nanofluids are situated in different computerized hardware, energy supply, energy age, air con and assembling. Vajjha and Das (2009) interestingly utilized EG (60 %) and water (40 %) total as base liquid for the readiness of alumina (Al2O3), copper oxide (CuO) and zinc oxide (ZnO) nanofluids. At the indistinguishable temperature and consideration, they saw that CuO nanofluid groups over the top warm conductivity assess to the ones of Al2O3 and ZnO nanofluids. Naik and Sundar (2011) took 70 % propylene glycol and 30 % water and arranged CuO nanofluid.

True to form, they found that CuO nanofluid has better warm conductivity and consistency homes contrast with base liquid. Malvandi et al.(2013) concentrated on entropy age of nanofluids over a plate systematically. They utilized the homotopy-pertubation strategy (HPM) and the variational cycle technique (VIM) to settle the nonlinear conventional differential condition. It was noticed that the high thickness of Cu added as nanoparticles to water produces more entropy rather than other nanoparticles in a cycle. Murugesan and Kumar.(2019) left on the review gooey dissemination and joule warming consequences for thermo solutal delineated nanofluid over an extending sheet. They commented that Schmidt number declines the temperature subsequent to getting a mathematical arrangement of the nonlinear conventional differential conditions. Khan et al.(2012) concentrated on the unstable mhd free convection of nanofluid along an extending sheet with warm radiation. They acquired different time steps and for the various upsides of the boundaries of physical and designing interest. Regular convection stream of fragmentary nanofluids over an isothermal vertical plate with warm radiation was concentrated by Constantin et al.(2017). The liquid temperature increments for expanding upsides of the nanoparticle volume division were noted by them subsequent to acquiring the shut structure arrangement and plotting the chart. Latiff et al.(2016) concentrated on Stefan blowing impact of nanofluid over a strong turning stretchable circle. The nonlinear standard differential conditions were settled mathematically utilizing the Runge-Kutta-Fehlberg strategy. It was commented that the Stefan blowing expands the neighborhood skin rubbing and diminishes the intensity move, mass exchange and microorganism move rates. Second request slip stream of Cu-Water nanofluid over an extending sheet with heat move was gone through by Rajesh et al.(2014). They tackled the differential conditions utilizing limited component strategy. They showed the impacts of boundaries variety with the guide of charts. Aaiza et al.(2015) concentrated on energy move in nanofluid containing various states of nanoparticles. They observed that thickness and warm conductivity are the most noticeable boundaries answerable for various consequences of speed and temperature.

Penetrable medium is a medium that has interconnected pores where fluids can travel through. It is significant as it is all around used in the strong protection of a few hidden pieces of turbojet and rocket engines, for instance, start chamber dividers, exhaust spouts or gas turbine sharp edges from hot gases. Eckert and Drake(1958) and Jain and Bansal(1973) depicted warmth move lessening of coutte stream of incompressible fluid imbued into the stream field from a plate that is fixed inverse the removal of warmth from a plate that is moving. It has a two layered issue in capsulated by uniform imbuement and pull applied at the porous plate. Gersten and Gross(1974) checked warmth move along a plane wall with periodic pull speed.

Magnetohydrodynamic (MHD) liquid is a liquid that conducts power in electric and attractive fields. It integrates liquid elements and electromagnetic statements to depict simultaneous impacts of attractive field on the stream as well as the other way around. Its anxiety is on gases that are ionized and fluids that are electrically leading. Assortments of papers have advanced throughout the long term on this idea. Take for example; Singh and Mathew(2008) concentrated on the impacts that infusion/pull has on swaying hydrodynamic attractive stream in an even channel that is turning. Attia and Kotb(1996) inspected magnetohydrodynamic stream between equal plates having heat move. Swapna et al.(2017) concentrated on mass exchange on blended convective occasional move through permeable medium in a slanted channel. Achogo et

al.(2020) inspected magnetohydrodynamic convective occasional course through a permeable medium in a slanted channel with warm radiation and compound response.

The idea of regular convective intensity move happens attributable to distinction in temperature in a nook or close to a warmed or cooled level plate. Much consideration has been given to normal convection on even and vertical channel yet a couple of considerations has been given to slanted plates notwithstanding the regular event of this mathematical design in designing and common habitat. Among the couple of specialists that made exploration on slanted surface are Ganesan and Palani(2003) and Sparrow and Husar(1969) who concentrated on normal convection on slanted plate. Said et al.(2005) researched fierce regular convection between slanted isothermal plates. Chen(2004) concentrated on normal convection stream over a slanted surface that is penetrable having variable wall temperature and fixation. Hossain et al.(1996) analyzed the free convection from developing from leaned at little point to the plate that is isothermal. The mathematical arrangement of free convection stream past a slanted surface was concentrated by Anghel et al.(2001). Precise arrangement examination of radiative convective progression of intensity and mass exchange over slanted plate in a permeable medium was inspected Bhuvaneswari et al.(2010) concluded MHD stream, intensity and mass exchange on a slanted extending sheet having warm radiation and corridor impact that is penetrable. Achogo et al.(2020) concentrated on common impacts of intensity and mass exchange on mhd move through a channel with occasional wall fixation and temperature.

The investigation of warm radiation in channels of various calculations has gotten consideration from specialists attributable to its importance in free convection which is helpful in the warming of rooms and structures by the utilization of radiators. Ahmed and Sarmah(2009) concentrated on warm radiation impact on a transient MHD stream with mass exchange past an indiscreetly fixed vertical plate. Alabraba et al.(1992) analyzed free convection cooperation with warm radiation in a hydrodynamic limit layer considering the paired compound response and the less gone to Soret and Dufour impacts. Alagoa et al.(1998) investigated the radiative and free convective impacts of a MHD course through a permeable medium between boundless equal plates with time-subordinate pull. Bestman(2005) concentrated on free convection heat move to consistent transmitting non - Newtonian MHD stream past an upward permeable plate. Cess(1966) concentrated on the connection of warm radiation with free convection heat move. Ghosh et al.(2010) researched the warm radiation impacts on unstable hydromagnetic gas stream along a slanted plane with aberrant normal convection. Israel Cookey et al.(2010) concentrated on MHD oscillatory Coutte stream of an emanating gooey liquid in a permeable medium with occasional wall temperature. Sharma et al.(2014) concentrated on radiative and free convective consequences for MHD move through a permeable medium with occasional wall temperature and intensity age or ingestion. Achogo et al.(2020) examined the impact of intensity source on mhd free convection through a channel with a wall having occasional temperature.

II. FORMULATION OF THE PROBLEM

We consider the periodic flow of an electrically conducting, viscous and incompressible silver water nanofluid through an inclined medium. The two plates are at a distance d apart. The coordinate system is chosen such that x – axis lies along the centerline and the y – axis along the magnetic field. The fluid is injected through the lower stationary porous plate and sucked through the upper porous plate in oscillatory motion in its own plane. The injection and suction

velocity is V'. The magnetic field is applied perpendicular to the parallel plates. The temperature difference of the plates is assumed high enough to induce radiation. All the physical parameters are independent of x for this problem of fully developed flows that is laminar. The flow is governed by the following equations:

$$\frac{\partial V'}{\partial y'} = 0 \tag{1}$$

$$\rho_{nf}\left(\frac{\partial u\prime}{\partial t\prime} + v'\frac{\partial u\prime}{\partial y\prime}\right) = -\frac{\partial p\prime}{\partial x\prime} + \mu_{nf}\frac{\partial^2 u\prime}{\partial y'^2} - \frac{\mu_{nf}}{K}u' - \sigma\beta_0^2 u' + g(\rho\beta)_{nf}T'\sin\propto$$
(2)

$$\left(\rho c_p\right)_{nf}\left(\frac{\partial T\prime}{\partial t\prime} + v'\frac{\partial T\prime}{\partial y\prime}\right) = k_{nf}\frac{\partial^2 T\prime}{\partial y'^2} - \frac{\partial q_r\prime}{\partial y\prime}$$
(3)

$$\left(\rho c_p\right)_{nf}\left(\frac{\partial C\prime}{\partial t\prime} + v'\frac{\partial C\prime}{\partial y\prime}\right) = D_{nf}\frac{\partial^2 C\prime}{\partial y'^2} \tag{4}$$

The boundary conditions expedient to this problem are

$$u' = 0,\ v' = V, T' = 0\ , C' = 0 \text{at y} = -\frac{d}{2} \tag{5a}$$

$$u' = \text{Ucos}\omega' t',\ v^I = V, T' = T_0\text{cos}\omega' t'\ , C' = C_0\text{cos}\omega' t' \text{at y} = \frac{d}{2}$$
(5b)

where $u'(y', t')$ axial velocity, t' is the time, ν' is the kinematic viscosity, σ is electrical conductivity, C_p is the specific heat at constant pressure, ρ is the fluid density, ω is the frequency of oscillation, $T'$is the temperature of the fluid, C' is the concentration of the fluid, B_0 is the magnetic field, T_0 is reference temperature, P' is the pressure, V is the oscillating velocity, g is the acceleration due to gravity, $K_r'$is the chemical reaction term, q' is the radiation flux, K' is the permeability of the porous medium, B_T is thermal volume expansion coefficient of nanofluid, $\left(\rho c_p\right)_{nf}$ the heat capacitance of nanofluids, k_{nf} the thermal conductivity of nanofluid, q_r the radiative heat flux in x-direction.

Following the Hamilton and Crosser model(1962),the dynamic viscosity of the nanofluid(μ_{nf}), thermal expansion coefficient of nanofluid($(\rho\beta)_{nf}$), heat capacitance of nanofluids($\left(\rho c_p\right)_{nf}$), thermal conductivity of nanofluid(k_{nf}) are;

$$\mu_{nf} = \mu_f(1 + a\emptyset + b\emptyset^2)$$
(6a)

$$\frac{k_{nf}}{k_f} = \frac{k_s + (n-1)k_f + (n-1)(k_s - k_f)\emptyset}{k_s + (n-1)k_f + (k_s - k_f)\emptyset}$$
(6b)

$$\rho_{nf} = (1-\emptyset)\rho_f + \emptyset\rho_s$$
(6c)
$$(\rho\beta)_{nf} = (1-\emptyset)(\rho\beta)_f + \emptyset(\rho\beta)_s$$
(6d)
$$(\rho c_p)_{nf} = (1-\emptyset)(\rho c_p)_f + \emptyset(\rho c_p)_s$$
(6e)

$\emptyset$ denotes the nanoparticles volume fraction, ρ_f and ρ_s are the densities of the base fluid and solid nanoparticles, β_s and β_f are the volumetric expansion coefficients of thermal expansions of solid nanopartiles and base fluids, $(c_p)_s$ and $(c_p)_f$ are the specific heat capacities of solid nanoparticles and base fluids at constant pressure, a and b represent constants and find their values on the particle shape as represented by Aaiza et al.(2015) in Table 1. The n in equation (4b) denotes the empirical shape factor and it is expressed as $n = \frac{3}{\Psi}$, where Ψ means the sphericity which denotes the ratio between the surface are of the sphere and the surface area of the real particle with equal volumes(Aiza et al.(2015)). The Ψ is clearly seen in Table 2.

Table1: Constants a and b empirical shape factors

Model	Platelet	Blade	Cylinder	Brick
A	37.1	14.6	13.5	1.9
B	612.6	123.3	904.4	471.4

Table 2: Sphericity Ψ for different shapes nanoparticles

Model	Platelet	Blade	Cylinder	Brick
Ψ	0.52	0.36	0.62	0.81

Table 3: Thermophysical properties of water and nanoparticles

Model	$\rho(kgm^{-3})$	$c_p(kg^{-1}K^{-1})$	$k(Wm^{-1}K^{-1})$	$\beta \times 10^{-5}(K^{-1})$
Pure water(H_2O)	997.1	4179	0.613	21
Copper(Cu)	10500	235	429	1.89

We assumed that the fluid is optically thin having a relatively low density. Hence the heat flux according to Cogley et al.(1968) is expressed as;

$$\frac{\partial q^{'}}{\partial y^{'}} = 4\alpha^{2}T^{'} \tag{7}$$

where α is the mean absorption coefficient.

Going by the internal flow of the oscillation in the channel; the pressure gradient variations is assumed as

$$-\frac{1}{\rho_f}\frac{\partial p^{'}}{\partial x^{'}} = P\cos\omega^{'}t^{'} \tag{8}$$

Substituting equation (7) into equation (3); we get

$$(\rho c_p)_{nf}\left(\frac{\partial T'}{\partial t'} + v'\frac{\partial T'}{\partial y'}\right) = k_{nf}\frac{\partial^2 T'}{\partial y'^2} - 4\alpha^2 T^{\iota} \quad (9)$$

Equation (1) integrates to $v' = V$ on the assumption that there is constant injection and suction velocity V at the upper and lower plates.

Introducing the following dimensionless variables equation (10):

$x = \frac{x'}{d}$, $y = \frac{y'}{d}$, $u = \frac{u'}{U}$, $Kr = \frac{K'd^2}{\vartheta}$,, $T = \frac{T'}{T_0}$,, $C = \frac{C'}{C_0}$, $v' = V$, $P = \frac{P'}{\rho_f UV}$, $\omega = \frac{\omega' d^2}{\vartheta_f}$, $t = \omega' t'$, $Re = \frac{Vd}{\vartheta_f}$,

$Pe_t = \frac{Vd(\rho C_p)_f}{k_f}$, $Pe_t = \frac{Vd(\rho C_p)_f}{D_{nf}}$, $k = \frac{K'}{d^2}$, $M^2 = \frac{\sigma B_0^2 d^2}{\mu_f}$, $N^2 = \frac{4\propto^2 d^2}{k_f}$, $Gr = \frac{g(B_T)_f T_0 d^2}{\mu_f \cup}$, $Gc = \frac{g(B_T)_f C_0 d^2}{\mu_f \cup}$,,

$\lambda = \frac{k_{nf}}{k_f}$

$$\rho_f = \frac{\mu_f}{\nu_f}, \quad (10)$$

and equations (6a-6e) into equations (2) -(9), we obtain

$$[1 - \phi + \phi\frac{\rho_s}{\rho_f}](\frac{\omega}{Re}\frac{\partial u}{\partial y} + \frac{\partial u}{\partial y}) = -\frac{\partial P}{\partial x} + \frac{(1+a\emptyset+b\emptyset^2)}{Re}\frac{\partial^2 u}{\partial y^2} - \frac{M^2}{Re}u - \frac{(1+a\emptyset+b\emptyset^2)}{kRe}u$$

$$+\left[(1-\phi)\rho_f + \phi\frac{(\rho\beta)_s}{(\beta)_f}\right]\frac{Gr}{Re}sin \propto T + \left[(1-\phi)\rho_f + \phi\frac{(\rho\beta)_s}{(\beta)_f}\right]\frac{Gm}{Re}sin \propto C$$

(11)

$$[1 - \phi + \phi\frac{(\rho c_p)_s}{(\rho c_p)_f}](\frac{\omega}{Re}\frac{\partial T}{\partial t} + \frac{\partial T}{\partial y}) = \frac{\lambda}{Pe}\frac{\partial^2 T}{\partial y^2} - \frac{N^2}{Pe}T$$

(12)

$$[1 - \phi + \phi\frac{(\rho c_p)_s}{(\rho c_p)_f}](\frac{\omega}{Re}\frac{\partial C}{\partial t} + \frac{\partial C}{\partial y}) = \frac{\lambda}{Pe_c}\frac{\partial^2 T}{\partial y^2} - \frac{KrSc}{Pe}C$$

(13)

where u is the dimensionless velocity, y is the dimensionless co-ordinate axis normal to the plates, t is the dimensionless time, T is the dimensionless temperature, Gr is the thermal Grashof number, Peclet number, M is the magnetic parameter, K porosity, λ the effective thermal conductivity, N radiation parameter, Re is the Reynolds number

The corresponding boundary conditions are non - dimensioned to;

$u = T = C = 0$ at $y = -\frac{1}{2}$ (14)

$u = T = C = 1$ at $y = \frac{1}{2}$ (15)

III. METHOD OF SOLUTION

Equations (10) – (13) are second order coupled partial differential equations, we therefore assumed the solution of the form;

$u(y) = u_0(y)e^{it}$ (16)

$T(y,t) = \theta_0(y)e^{it}$ (17)

$C(y,t) = \emptyset_0(y)e^{it}$ (18)

$-\frac{\partial P}{\partial x} = Pe^{it}$ (19)

Applying (15 –17) into the relevant equations in (11 - 14), we obtain

$$\frac{d^2u_0}{dy^2} - \frac{Rem_3}{m_4}\frac{du_0}{dy} - \left(\frac{M^2}{m_4} + \frac{I}{K} + \frac{i\omega m_3}{m_4}\right)u_0 = \frac{-ReP}{m_4} - \frac{Grm_5}{m_4}\sin\propto\theta_0 + \frac{Gmm_5}{m_4}\sin\propto\emptyset_0 \quad (20)$$

$$\frac{d^2\theta_0}{dy^2} - \frac{Pe_t m_1}{\lambda}\frac{d\theta_0}{dy} - \left(\frac{N^2}{\lambda} + \frac{i\omega Pe_t m_1}{\lambda Re}\right)\theta_0 = 0 \quad (21)$$

$$\frac{d^2\emptyset_0}{dy^2} - m_1\frac{d\theta_0}{dy} - \left(ScKr + \frac{i\omega Pe_c m_1}{Re}\right)\emptyset_0 = 0 \quad (22)$$

where $m_3 = 1 - \phi + \phi\frac{\rho_s}{\rho_f}$, $m_4 = 1 + a\emptyset + b\emptyset^2$, $m_3 = (1-\phi)\rho_f + \phi\frac{(\rho\beta)_s}{(\beta)_f}$,

$$m_1 = 1 - \phi + \phi\frac{(\rho c_p)_s}{(\rho c_p)_f}$$

Subject to:

$u_0 = \theta_0 = \emptyset_0 = 0$ at $y = -\frac{1}{2}$ (23)

$u_0 = \theta_0 = \emptyset_0 = 1$ at $y = \frac{1}{2}$ (24)

Equations (20)- (22) are ordinary second order coupled differential equations and solved under the boundary conditions (23) and (24) corresponding to them through a straight forward analytical method, we obtain u(y) and $\theta_0(y)$ as

$$u_0(y) = D_5e^{\propto_5 y} + D_6e^{\propto_6 y} + D_7 + D_8e^{\propto_1 y} + D_9e^{\propto_2 y + \frac{\alpha_2 - \alpha_1}{2}} + D_{10}e^{\propto_3 y} + D_{11}e^{\propto_4 y + \frac{\alpha_4 - \alpha_3}{2}} \quad (25)$$

$$\theta_0(y) = A_1\left(e^{\propto_1 y} - e^{\propto_2 y + \frac{\alpha_2 - \alpha_1}{2}}\right) \quad (26)$$

$$\emptyset_0(y) = A_2\left(e^{\propto_3 y} - e^{\propto_4 y + \frac{\alpha_4 - \alpha_3}{2}}\right) \quad (27)$$

The final expressions of u(y,t), T(y,t) and C(y,t) are given by imputing equations(25-27) into equations(16-18)

$$u(y,t) = (D_5 e^{\propto_5 y} + D_6 e^{\propto_6 y} + D_7 + D_8 e^{\propto_1 y} + D_9 e^{\propto_2 y + \frac{\alpha_2 - \alpha_1}{2}} + D_{10} e^{\propto_3 y} + D_{11} e^{\propto_4 y + \frac{\alpha_4 - \alpha_3}{2}}) e^{it} \quad (28)$$

$$T(y,t) = \left[A_1 (e^{\propto_1 y} - e^{\propto_2 y + \frac{\alpha_2 - \alpha_1}{2}})\right] e^{it} \quad (29)$$

$$C(y,t) = \left[A_2 (e^{\propto_3 y} - e^{\propto_4 y + \frac{\alpha_4 - \alpha_3}{2}})\right] e^{it} \quad (30)$$

The values for A1, A2 , D3 to D11 and $\propto_1 \ to \ \propto_6$ are not given for brevity.

The physical point of expression for the shear stress, Nusselt number and the Sherwood number on the walls are given below

$$\tau = \left(\frac{\partial u_0}{\partial y}\right)_{y=0} = \propto_5 D_5 + \propto_6 D_6 + \propto_1 D_8 + \propto_2 D_9 + \propto_3 D_{10} + \propto_4 D_{11} \quad (31)$$

$$Nu = -\left(\frac{\partial \theta_0}{\partial y}\right)_{y=0} = -A_1(\propto_1 + \propto_2) \quad (32)$$

$$Sh = -\left(\frac{\partial \emptyset_0}{\partial y}\right)_{y=0} = -A_2(\propto_3 + \propto_4) \quad (33)$$

IV. RESULTS AND DISCUSSION

Figure 1 depicts the effect of Peclet number on the temperature profile. It is clearly seen that increasing the Peclet number fosters a decrease in the temperature of the fluid. There is no significant change in the temperature profile with consequential increase in the Reynolds number as shown in figure 3. It is shown clearly in figure 5 that increasing the volume fraction produces no change in the temperature of the fluid. Increasing the effective thermal conductivity of the nanofluid produces an increase in the temperature of the nanofluid as shown in figure 4. The thermal radiation is shown in figure 2. It is shown that increasing the thermal radiation of the nanofluid; consequentially decreases the temperature of the nanofluid. This physically true because radiating energy at higher values reduces the temperature of the nanofluid. This results also agrees with the result obtained by Aaiza et al.(2015). The variation of the frequency of oscillation produces no significant change in the temperature of the nanofluid in figure 6. In figure 12, the increase in the Peclet number produces a corresponding increase in the velocity profile of the nanofluid. The effect of the increase in the Reynolds number on the velocity is shown in figure 14. From figure 14, it is seen that there is a corresponding increase in the velocity profile. This result is consistent with the result obtained by Ngiangia and Akaezue (2019). It shows that increasing the volume fraction consequentially increase the velocity of the nanofluid as depicted in figure 16. This consistent with the result obtained by Aaiza et al.(2015).

It is also seen that the effective thermal conductivity increases the velocity of the fluid when being increased as displayed in figure 10. Figure 13 shows the effect of thermal radiation on the velocity profile. It is seen that increasing the thermal radiation consequentially reduces the velocity of the nanofluid. This is true because thermal radiatioin leads to a reduction in the momentum boundary layer. This is consistent with the result obtained by Achogo et al.(2020). There is no change in the velocity of the nanofluid for an increase in the frequency of oscillation as shown in figure 17. Take notice that figure 21 shows the effect of the magnetic parameter on the velocity profile. The figure shows that increasing the magnetic parameter leads to a reduction in the velocity of the nanofluid. This is so owing to the presence of Lorentz force in the magnetic field. Aaiza et al.(2015) obtained similar result. Figure 24 shows the impact rendered on the velocity profile by varying the porosity or permeability. Permeability is a property of the porous medium. Hence, increasing the permeability leads to an increase in the velocity since it results in the ability of the formation to transfer more fluid. The effect of the thermal Grashof number is shown in figure 22 and 23. Increasing the Grashof number leads to an increase in the velocity profile. It is physically true since thermal buoyancy leads to an increase in the boundary layer. Aaiza et al.(2015) obtained the same result as this. It is seen clearly in figure 7 an increase and decrease at the lower and upper plate of the concentration of the fluid with i9ncrerase in the Peclet number due to concentration. Increasing the Schmidt number produces a decrease in the contraction fo the fluid in figure 9. No change is noted in the concentration for the fluid with increase in the Reynolds number and volume fraction respectively as depicted in figure 7 and 10. Increasing the frequency of oscillation decrease the concentration of the fluid in figure 8 and 11 respectively. A decrease in the velocity of the fluid with increase in the Peclet number due to temperature and concentration as seen in figure 18 and 12. The pick is high at the upper plate than at the lower plate.increasing the chemical reaction, Peclet number and Schmidt number decrease the velocity of the fluid as noted in figure 18, 19 and 20 with the pick being more at the upper plate. In figure 26, it is seen that the shape factor decrease the velocity of the fluid with increase in it.

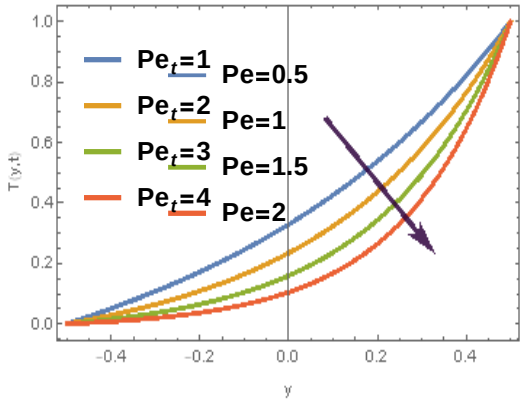

Figure 1: Dependence of Temperature profile on coordinate with Peclet number due to temperature varying

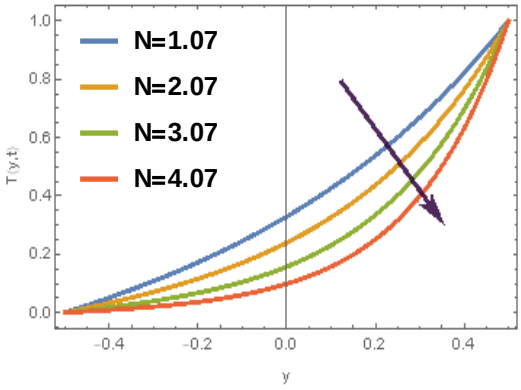

Figure 2: Dependence of Temperature profile on coordinate with thermal radiation varying

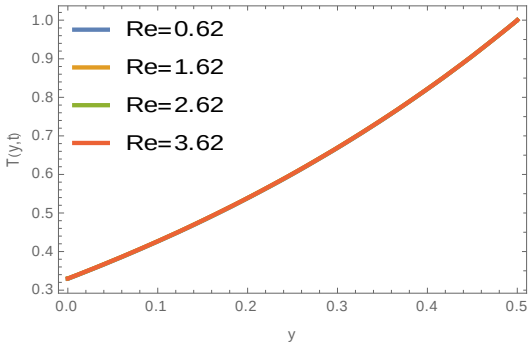

Figure 3: Dependence of Temperature profile on coordinate with Reynolds number varying

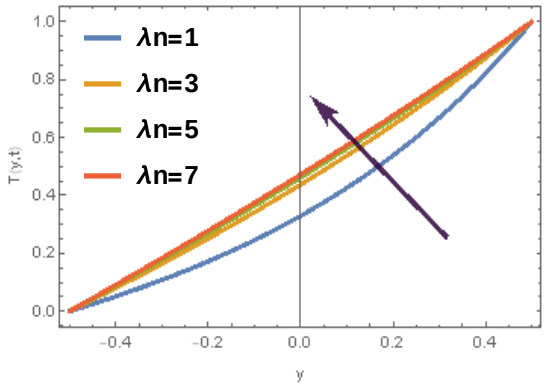

Figure 4: Dependence of Temperature profile on coordinate with thermal conductivity varying

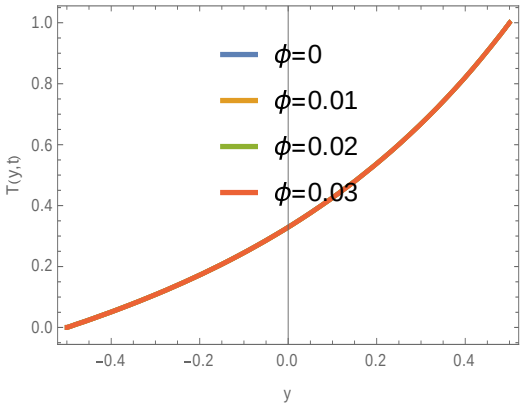

Figure 5: Dependence of Temperature profile on coordinate with volume fraction varying

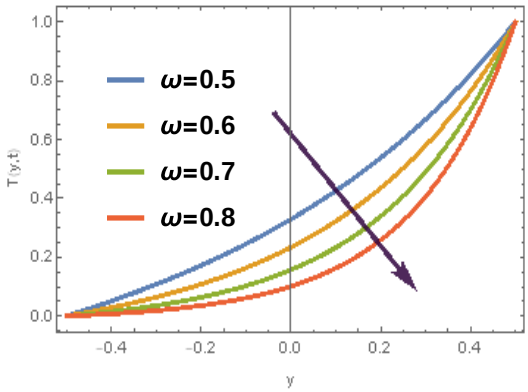

Figure 6: Dependence of Temperature profile on coordinate with frequency of oscillation varying

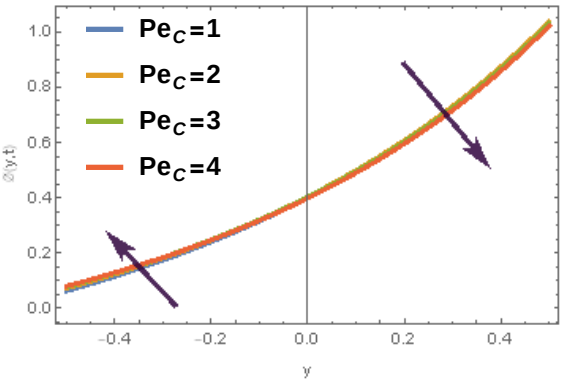

Figure 7: Dependence of Concentration profile on coordinate with Peclet number due to concentration varying

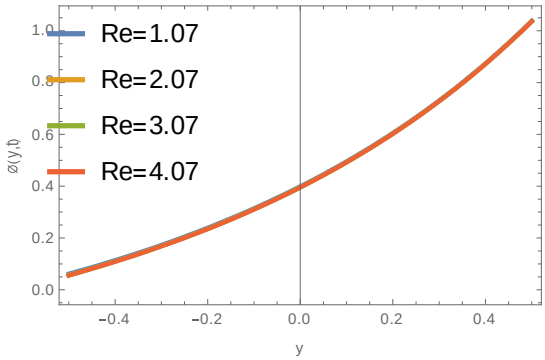

Figure 8: Dependence of Concentration profile on coordinate with Reynolds number varying

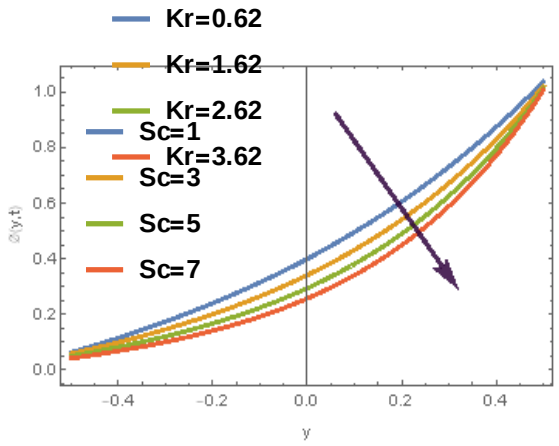

Figure 10: Dependence of Concentration profile on coordinate with Schmidt number varying

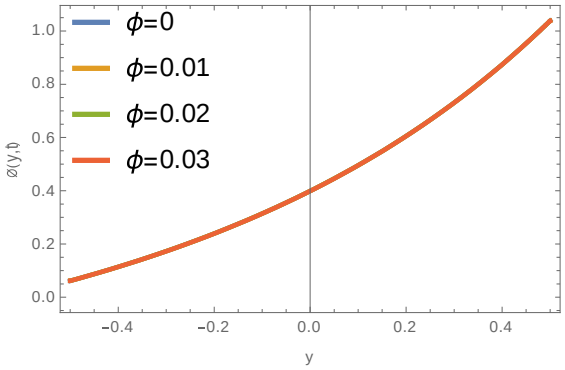

Figure 11: Dependence of Concentration profile on coordinate with volume fraction varying

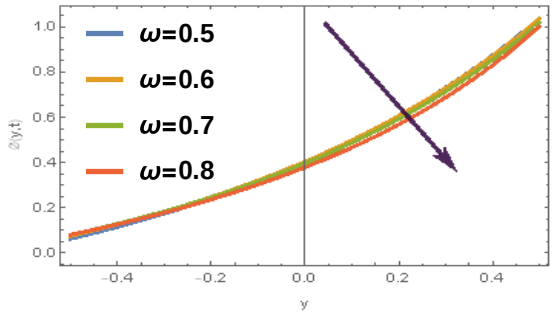

Figure 12: Dependence of Concentration profile on coordinate with frequency of oscillation varying

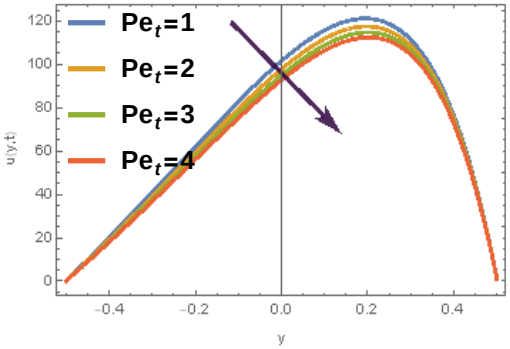

Figure 13: Dependence of velocity profile on coordinate with Peclet number due to temperature varying

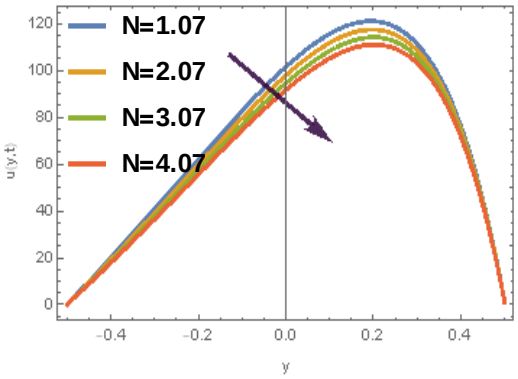

Figure 14: Dependence of velocity profile on coordinate with thermal radiation varying

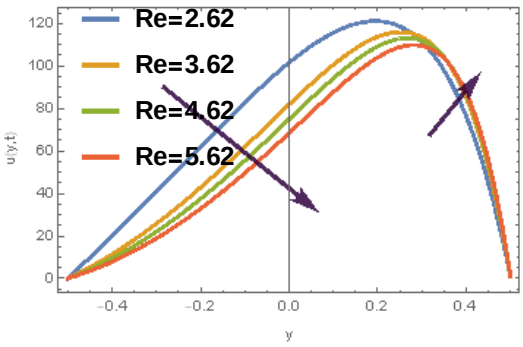

Figure 15: Dependence of velocity profile on coordinate with Reynolds number varying

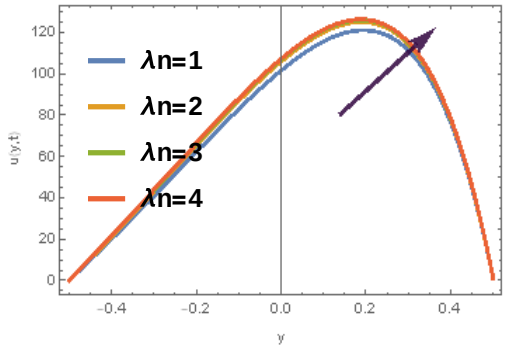

Figure 16: Dependence of velocity profile on coordinate with thermal conductivity varying

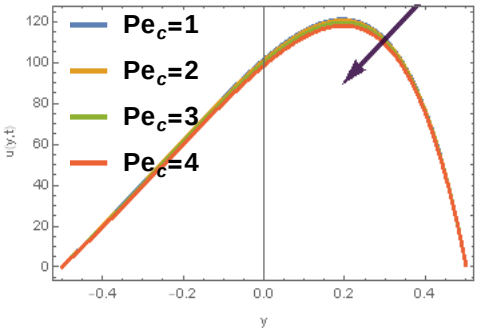

Figure 19: Dependence of velocity profile on coordinate with Peclet number due to concentration varying

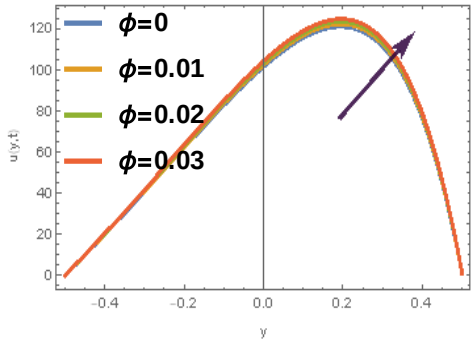

Figure 17: Dependence of velocity profile on coordinate with volume fraction varying

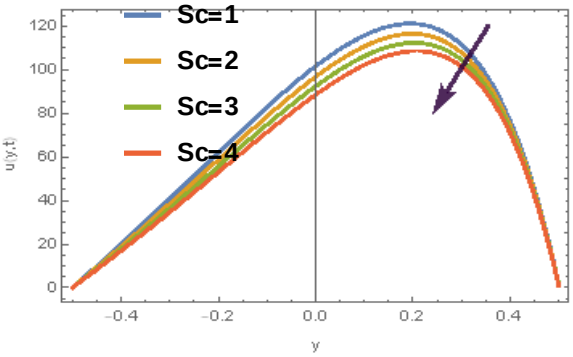

Figure 21: Dependence of velocity profile on coordinate with Schmidt number varying

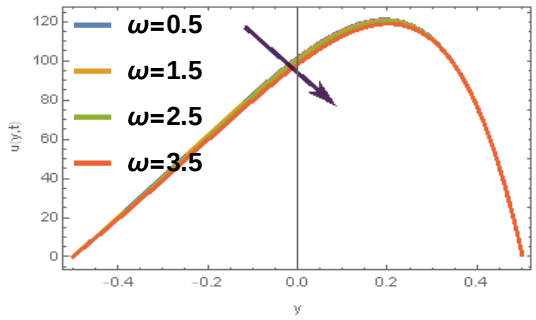

Figure 18: Dependence of velocity profile on coordinate with frequency of oscillation varying

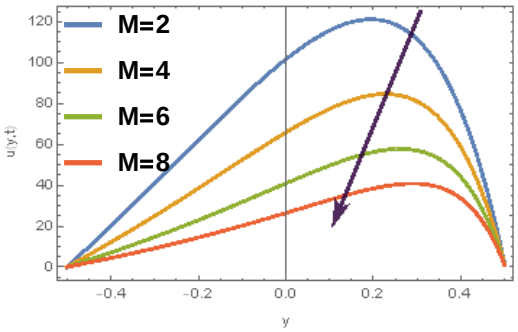

Figure 22: Dependence of velocity profile on coordinate with Harttman number varying

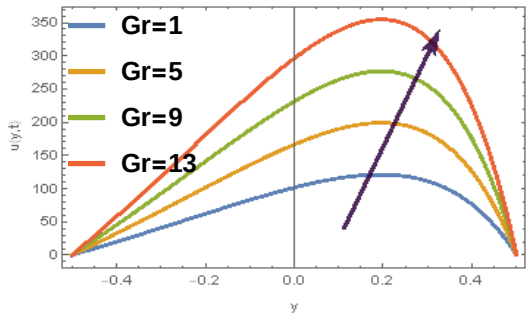

Figure 22: Dependence of velocity profile on coordinate with Thermal Grashof number varying

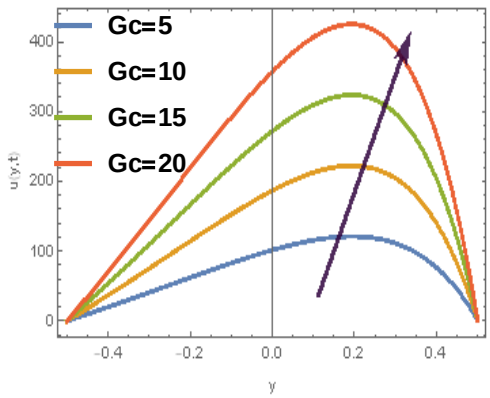

Figure 24: Dependence of velocity profile on coordinate with Solutal Grashof number varying

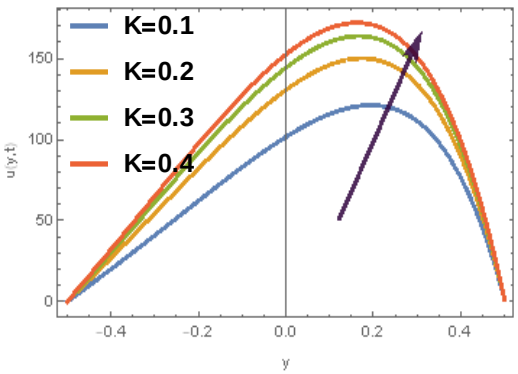

Figure 25: Dependence of velocity profile on coordinate with Porosity varying

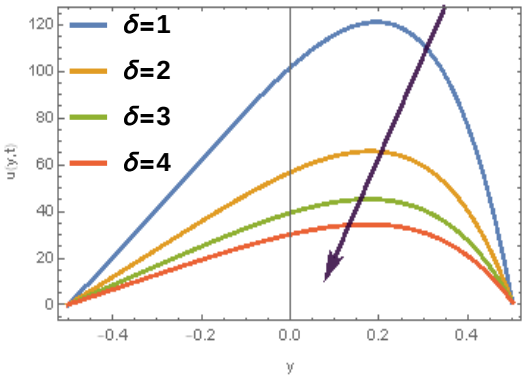

Figure 26: Dependence of velocity profile on coordinate with shape factor varying

V. CONCLUSIONS

In this paper, we have studied the impact of transpiration cooling on oscillatory mhd convection of ag-water nanofluid through an inclined permeable channel. The governing equations were solved using analytical approach and the solutions obtained were expressed in terms of exponential functions. From the study, the following have been drawn.

1. Increasing the effective thermal conductivity causes an increase in the temperature of the nanofluid.
2. Increasing the thermal radiation consequentially reduces the temperature of the nanofluid.
3. An increase in the Peclet number causes an increase in the temperature of the nanofluid.
4. Increase in the Reynolds number increases the velocity of the nanofluid.
5. Increase in the thermal radiation reduces the velocity of the nanofluid.
6. Increasing the Harttman number correspondingly reduces the velocity of the nanofluid.
7. Increase in the porosity causes an increase in the velocity of the nanofluid.
8. Increase in the thermal Grashof number increases the velocity of the nanofluid.

REFERENCES

Aaiza, G.; Khan, I & Shafie, S.(2015). Energy transfer in mixed convection MHD flow of nanofluid containing different shapes of nanoparticles in a channel filled with saturated porous medium. *Nanoscale research letters,2*(2015), 1-16.

Achogo W. H. & Adikabu I. N.(2020). Mutual influences of heat and mass transfer on mhd flow through a channel with periodic wall concentration and temperature. *International journal of research and innovation in applied science,5*(6):2454-6194.

Achogo W. H., Okereke I. C. Ofomata A. I. & Amadi O. F.(2020) .Magnetohydrodynamic convective periodic flow through a porous medium in an inclined channel with thermal radiation and chemical reaction. *International Journal of Innovative Science and Research Technology,5*(1):1129-1139.

Achogo W. H., Okereke I. C. Ofomata A. I. & Eleonu B. C.(2020) .Effect of heat source on Magnetohydrodynamic free convection through a channel with a wall having periodic temperature. *International Journal of Innovative Science and Research Technology,5*(4):1035-1040.

Ahmed, N. & Sarmah, H. K. (2009). Thermal radiation effect on a transient MHD flow with mass transfer past an impulsively fixed infinite vertical plate. *Internatiional Journal of Applied Mathematics and Mechanics, 5*(5) 87-98.

Alabraba, M. A.;Bestman, A. R. & Ogulu, A. (1992). Free convection interaction with thermal radiatin in a hydromangetic boundary layer taking into account the binary chemical reaction and the less attended Soret and Dufour effects.*Astrophysics Space Science,195*(1992), 431-445.

Alagoa, K. D.; Tay, G. & Abbey, T. M. (1998). Radiative and free convective effects of a MHD flow through a porous medium between infinite parallel plates with time – dependent suction. *Astrophysics and Space Science, 260*(1998),455-468.

Anghel M., Hossain M. A. & Zeb S. (2001). Combined heat and mass transfer by free convection past an inclined flat plate. *International Journal Applied Mechanics and Engineering,2*(2001), 473-497.

Attia H. A. & Kotb N. A. (1996). MHD flow between two with heat transfer parallel plates. *ActaMechanica, 117*(1996), 215-220.

Bestman, A. R. (2005). Free convection heat transfer to steady radiating non – Newtonian MHD flow past a vertical porous plate. *International Journal Numerical Methods in engineering, 21*(2005) 899 – 908.

Bhuvaneswari M. & Sivasankaran S., Kim Y. J. (2010). Exact analysis of radiation convective flow heat and mass transfer over an inclined plate in a porous medium.", *World Applied Journal, 10*(2010),774-778

Cess, R. D. (1966). The interaction of thermal radiation with free convection heat transfer..*Int. J. Heat and Mass Transfer,9*(1996),1269-1277.

Chen C.H,(2004). Heat and mass transfer in MHD flow with variable wall temperature and concentration, *ActaMechanica, 172* (2004),219-235.

Choi SUS (1995). Enhancing thermal conductivity of fluids with nanoparticle, in: D.A. Siginer, H.P. Wang (Eds.), Developments and Applications of Non- Newtonian Flows. ASME FED, *66*(1995),99–105.

Constantin F.; Dumitru V. & Waqas A. A.(2017). Natural convection flow of fractional nanofluids over an isothermal vertical plate with thermal radiation. *Applied Sciences,7*(247),1-13. DOI:10.3390/app7030247

Eckert, E. R. G. & Drake R. M. (1958). *Heat and Mass Transfer*. McGrawHill Book Co., New York.

Ganesan P & Palani G. (2003). Natural convection effects on impulsively started inclined plate with heat and mass transfer. *Heat and Mass Transfer, 39* (2003), 277-283.

Gersten K. and J.F. Gross J. F. (1974). Flow and heat transfer along a plane wall with periodic suction. *Mathematical Physics,25*(1974), 399-408.

Ghosh, S. K.; Rawat, S.; Beg, O. A. & Beg, T. A. (2010). Thermal radiation effects on unsteady hydromagnetics gas flow along an inclined plane with indirect natural convection. *International Journal of Applied Mathematics and Mechanics*, *6*(2010), 41 – 57.

Hamilton R. L. & Cross O. K.(1962). Thermal conductivity of heterogeneous two-component systems. *Journal of industrial & engineering chemistry fundamentals,1*(1962),187-191.

Hossain M. A., I. Pop I. & Ahmad M. (1996). MHD free convection flow from an isothermal plate. *International Theoretical & Applied Mechanics, 1*(1996), 194-207.

Israel-Cookey, C.; Amos, E. & Nwaigwe, C. (2010). MHD oscillatory Couette flow of a radiating viscous fluid in a porous medium with periodic wall temperature. *Journal of Science Industrial Research,1*(2) 326 – 331.

Jain N. C. & Bansal J. L., (1973). Couette flow with transpiration cooling when the viscosity of the fluid depends on temperature. *Proceeding Indian Academic Science,77*(1973), 184-200.

Khan, S. M.; Karim, I; Ali, E. L. & Islam, A.(2012). Unsteady MHD free convection boundary – layer flow of a nanofluid along a stretching sheet with thermal radiation and viscous dissipation effects. *International nano letters, 2*(2012), 1-9.

Latiff, N. A.; Uddin, M. J. & Ismail, A. I.(2016). Stefan blowing effect on bioconvective flow of nanofluid over a solid rotating stretchable disk. Propulsion and power research, 5(4), 267-278.

Malvandi, A.; Ganji, D. D.; Hedayati, F & Rad, Y. E.(2013). An analytical study on entropy generation of nanofluids over a flat plate. *Alexandria engineering journal, 52* (2013), 595-604.

Mohammed R. A.(2009). Double –Diffusioin convection-radiation interaction on Unsteady MHD flow over a vertical moving porous plate with heat generation and soret effects. Applied Mathematical Sciences, *3*(13),629-651.

Murugesan, T. & Kumar, D. M.(2019). Viscous dissipation and joule heating effects on MHD flow of a thermo-solutal stratified nanofluid over an exponentially stretching sheet with radiation and heat generation/absorption. *World schientific news, 129*(2019),193-210.

Naik, M. T. & Sundar, L. S. (2011). Investigation into thermophysical properties of glycol based CuO nanofluid for heat transfer applications. World AcadScience Engineer Technology, *59*(2011),,440–446.

Said S.A.M., Habib M.A., Badr H.M. & Anwar S. (2005). Turbulent natural convection between inclined isothermal plates, *Computers and Fluid*, *34*(9) 1025-1039.

Sharma R. & Isahk, A.(2014). Second order slip flow of Cu-Water nanofluid over a stretching sheet with heat transfer. WSEAS transactions on fluid mechanics, 9(2014), 26-33.

Singh K. D. & Mathew A. (2008). Injection/suction effects on an oscillatory hydromagnetic flow in a rotating horizontal porous channel. *Indian Journal Physics,82*(4), 435-445.

Swapna Y., M. C. Raju & Ram Prakash Sharma (2017). Mass transfer effects on MHD mixed convective periodic flow through porous medium in an inclined channel with transpiration cooling and thermal radiation. *Jnananbha,47*(1), 195 – 206.

Vajjha, R.S. & Das, D.K .(2009). Experimental determination of thermal conductivity of three nanofluids and development of new correlations. *International journal of heat and mass transfer*, *52*(2009), 4675-4682.

Appendix

$$D_5 = A_3[1 + D_7 e^{\alpha_6} + D_8 e^{\frac{2\alpha_6-\alpha_1}{2}} + D_9 e^{\frac{2\alpha_6-\alpha_1}{2}} + D_{10} e^{\frac{2\alpha_6-\alpha_3}{2}} + D_{11} e^{\frac{2\alpha_6-\alpha_3}{2}} - D_7 - D_8 e^{\frac{\alpha_1}{2}} - D_9 e^{\frac{2\alpha_2-\alpha_1}{2}} - D_{10} e^{\frac{\alpha_3}{2}} - D_{11} e^{\frac{2\alpha_4-\alpha_3}{2}}]$$

$$D_6 = -A_3\left[1 + D_7 e^{\alpha_6} + D_8 e^{\frac{2\alpha_6-\alpha_1}{2}} + D_9 e^{\frac{2\alpha_6-\alpha_1}{2}} + D_{10} e^{\frac{2\alpha_6-\alpha_3}{2}} + D_{11} e^{\frac{2\alpha_6-\alpha_3}{2}} - D_7 - D_8 e^{\frac{\alpha_1}{2}} - D_9 e^{\frac{2\alpha_2-\alpha_1}{2}} - D_{10} e^{\frac{\alpha_3}{2}} - D_{11} e^{\frac{2\alpha_4-\alpha_3}{2}}\right] e^{\frac{\alpha_6-\alpha_5}{2}} - D_7 e^{\frac{\alpha_6}{2}} - D_8 e^{\frac{\alpha_6-\alpha_1}{2}} - D_9 e^{\frac{\alpha_6-\alpha_1}{2}} - D_{10} e^{\frac{\alpha_6-\alpha_3}{2}} - D_{11} e^{\frac{2\alpha_6-\alpha_3}{2}}$$

$$A_1 = \frac{1}{e^{\frac{\alpha_2}{2}} - e^{\frac{2\alpha_1-\alpha_2}{2}}}, A_2 = \frac{1}{e^{\frac{\alpha_3}{2}} - e^{\frac{2\alpha_4-\alpha_3}{2}}}, A_3 = \frac{1}{e^{\frac{\alpha_5}{2}} - e^{\frac{2\alpha_6-\alpha_5}{2}}}, \alpha_1 = \frac{\frac{Pe_t m_1}{\lambda} + \sqrt{\left(\frac{Pe_t m_1}{\lambda}\right)^2 + 4\left(\frac{N^2}{\lambda} + \frac{i\omega Pe_t m_1}{\lambda}\right)}}{2}, \alpha_2 = \frac{\frac{Pe_t m_1}{\lambda} - \sqrt{\left(\frac{Pe_t m_1}{\lambda}\right)^2 + 4\left(\frac{N^2}{\lambda} + \frac{i\omega Pe_t m_1}{\lambda}\right)}}{2}$$

$$, \alpha_3 = \frac{m_2 + \sqrt{(m_2)^2 + 4\left(Sc + \frac{Pe_c i\omega m_2}{Re}\right)}}{2}, \alpha_4 = \frac{m_2 - \sqrt{(m_2)^2 + 4\left(Sc + \frac{Pe_c i\omega m_2}{Re}\right)}}{2}, \alpha_5 = \frac{\frac{Rem_3}{m_4} + \sqrt{\left(\frac{Rem_3}{m_4}\right)^2 + 4\left(\frac{1}{K} + \frac{i\omega m_3}{m_4} + \frac{M^2}{m_2}\right)}}{2}, \alpha_6 = \frac{\frac{Rem_3}{m_4} - \sqrt{\left(\frac{Rem_3}{m_4}\right)^2 + 4\left(\frac{1}{K} + \frac{i\omega m_3}{m_4} + \frac{M^2}{m_2}\right)}}{2}, D_7 = \frac{PRe}{m_4\left(\frac{1}{K} + \frac{i\omega m_5}{m_4} + \frac{M^2}{m_4}\right)}, D_8 = \frac{-\frac{m_5}{m_4} Gr sin\alpha A_1}{{\alpha_1}^2 - \frac{Rem_5\alpha_1}{m_4} - \left(\frac{1}{K} + \frac{i\omega m_5}{m_4} + \frac{M^2}{m_4}\right)}, D_9 = \frac{\frac{m_5}{m_4} Gr sin\alpha A_1}{{\alpha_2}^2 - \frac{Rem_5\alpha_2}{m_4} - \left(\frac{1}{K} + \frac{i\omega m_5}{m_4} + \frac{M^2}{m_4}\right)}, D_{10} = \frac{-\frac{m_5}{m_4} Gc sin\alpha A_2}{{\alpha_3}^2 - \frac{Rem_5\alpha_3}{m_4} - \left(\frac{1}{K} + \frac{i\omega m_5}{m_4} + \frac{M^2}{m_4}\right)}, D_{11} = \frac{\frac{m_5}{m_4} Gc sin\alpha A_2}{{\alpha_4}^2 - \frac{Rem_5\alpha_4}{m_4} - \left(\frac{1}{K} + \frac{i\omega m_5}{m_4} + \frac{M^2}{m_4}\right)},$$]